Minkowski diagram in relativity and holography

Nils Abramson

Now that ultrashort laser pulses can be used in holography, the temporal and spatial resolution approach the same order of magnitude. In that case the limited speed of light sometimes causes large measuring errors if correction methods are not introduced. Therefore, we want to revive the Minkowski diagram, which was invented in 1908 to visualize relativistic relations between time and space. We show how this diagram in a modified form can be used to derive both the static holodiagram, used for conventional holography, including ultrahigh-speed recordings of wavefronts, and a dynamic holodiagram used for studying the apparent distortions of objects recorded at relativistic speeds.

I. Introduction

The holodiagram[1] is a tool used for evaluation and visualization of the interferometric sensitivity in both classical and holographic interferometry. The desensitizing factor of the holodiagram (k) has the same influence as an apparent red shift of the light. (One interference fringe represents a distance of k 0.5λ, where $k = 1/\cos\alpha$, and α is half of the angle separating illumination and observation direction.) When picosecond laser pulses are studied it is found that again, the k value is a measure of an apparent lengthening of the pulse. In both cases the desensitizing of measurements based on wavelength or pulse length is caused by the angular separation of the point source of illumination from the point of observation.

If this separation is not caused by a fixed distance but instead by a velocity in relation to the measured object of the one who makes the measurement, the resulting desensitizing factor will still be the same.[2] Thus the k value of the holodiagram can also be used to evaluate and visualize relativistic effects like the Lorentz contraction and refer them to an apparent red shift or lengthening of the measuring rods. It is interesting, however, that in this way we find that the Lorentz contraction is only one special case of more general apparent elongations and contractions of fast moving objects.[3]

The author is with Royal Institute of Technology, Industrial Metrology, 10044 Stockholm 70, Sweden.

II. Minkowski Diagram

The reason such different phenomena as holographic interferometry and special relativity can use the same tool for visualization is perhaps best explained by the Minkowski diagram.[4,5] This diagram was designed in 1908 to visualize relativistic deformations of time and space in a graphic way. It is based on a light cone and its intersections with planes representing space. The inclination of these planes represent velocity and thus it is easy to understand that a moving circle is transformed to an ellipse or a sphere to an ellipsoid. By introducing a second cone, the light cone of observation we can, in a geometrical way, produce not only the ellipsoids of the holodiagram but also the ellipsoids of observation[3] that explain the accepted relativistic Lorentz contraction and also a number of other apparent deformations of space and time. Our method is based on first transforming a fixed coordinate system to the reference frame of a moving observer, whereafter his measuring results are transformed back again. Thus, we who are stationary judge how a moving observer judges our stationary world.

Let us study the original Minkowski diagram of Fig. 1. The x and y axes of the coordinate system represent two dimensions of our ordinary world, while the z axis represents time (t), multiplied by the speed of light (c), just to make the scales of time and space of the same magnitude. Thus in the x–ct coordinate system the velocity of light is represented by a straight line at 45° to the ct axis. As all other possible velocities are lower than that of light, they are represented by straight lines inclined at an angle of less than 45° to the ct axis.

A. Illumination

A point source of light (A) is situated at the center (O,O,O) of the coordinate system of Fig. 1. A spherical wavefront is emitted in all directions and expands with
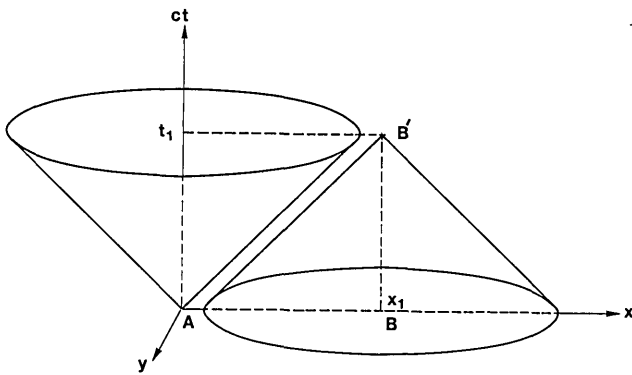
Fig. 1. Minkowski diagram. The x and y axes represent two dimensions of our ordinary world, while the vertical z axis represents time multiplied by the speed of light. Any constant velocity is represented by an inclined line inside the cone representing the speed of light. Thus, the expansion of a spherical wavefront is represented by a cone with its apex at the light source A. A converging spherical wavefront is represented by another, inverted cone with its apex at the point of observation B', separated from A by x_1. The two cones are out of contact because x_1 is larger than ct_1. This situation corresponds to a picosecond pulse of light emitted by A and a picosecond observation is, after a time delay of t_1, made at B'. No light is seen because the observation was made before the light arrived.
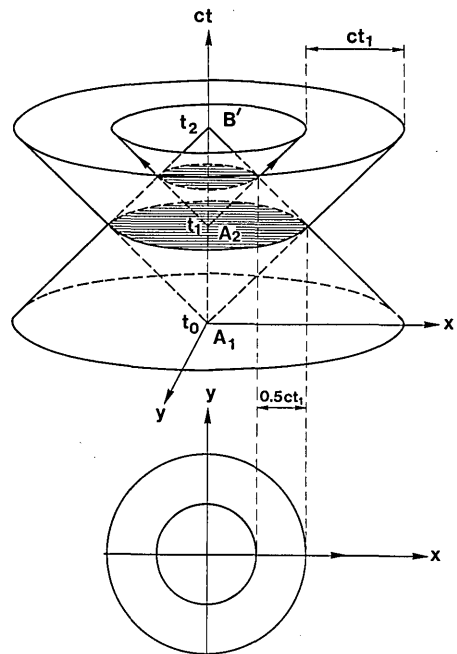

Fig. 2. Illumination and observation cones are separated in time but not in space. Two picosecond pulses are emitted at times t_0 and t_1, whereafter finally an observation is made at t_2. Light can be transmitted from illumination to observation cones only by scattering objects situated at the circular intersections of the cones. These circles have half of the radius of the cones at the time of observation (t_2). In our ordinary world this indicates that scattering or reflecting objects are seen only at a spherical surface that has half of the radius of the true spherical wavefront. Examples of this situation are radar and conventional interferometry where one fringe represents half of the wavelength.

the speed of light. In our chosen coordinate system, which is limited to only two space coordinates and one time coordinate, this phenomenon is represented by a cone with its apex at A, expanding in the direction of the positive time axis. Since no signal can be sent faster than light, no information from A can reach outside this cone that has an apex angle of 90°. The passing of time is represented by cross sections of the cone by planes parallel to the x-y plane at increasing ct values. These intersections will, when projected down to the x-y plane, produce circles of increasing radius that in out 3-D world represent the expanding spherical wavefront from the point source at A.

B. Observation

If a point of illumination represents a point source of light, a point of observation represents a point sink of light, a point toward which spherical waves are shrinking. In the Minkowski diagram it is represented by a cone that is inverted in relation to the light cone, referred to as the observation cone (B in Fig. 1), which like the light cone has a cone angle of 90° and where the observer is at the apex (B'). Thus an observer at B' can see nothing outside this cone because of the limited speed of light (c).

C. Light Transmitted to the Observation Cone

Now let us study the light cone and the observation cone used in a system for measurements based on, e.g., conventional interferometry, radar, gated viewing, holographic interferometry, holographic contouring using two frequencies or limited coherence length or short pulses of light (light-in-flight recording by holography).[6] All these methods are based on one point of illumination (A), one point of observation (B), object points (C), and a time delay.

D. Separation in Time but not in Space

The point source (A) produces two picosecond pulses of light at (O,O,O) and (O,O,t_1), respectively. Thereafter one single picosecond observation (B) is made at (O,O,t_2). The time separations of t_0, t_1, and t_2 are all dt. The result is seen in Fig. 2. Two concentric light cones are intersected by one observation cone. The intersections consist of two concentric circles in space (the x-y plane) with radii of $c\, dt$ and $0.5c\, dt$, respectively. They are thus separated in space by $0.5c\, dt$. Their time separation is $0.5dt$. Thus, to the observer the apparent radii and separation of the circles are half of their true value at the time of observation (t_2) as seen in Fig. 2.

This fact represents in our 3-D world that, for a certain time delay between illuminating pulse and observation, the object points that are seen are situated halfway out to the true wavefront. The reason is, of course, that to see an object point, light has to go twice the radius, out to the object and back again. The circles are separated in time by $0.5dt$, which corresponds to the fact that objects situated further away from the observer are seen as they were at an earlier point of time.
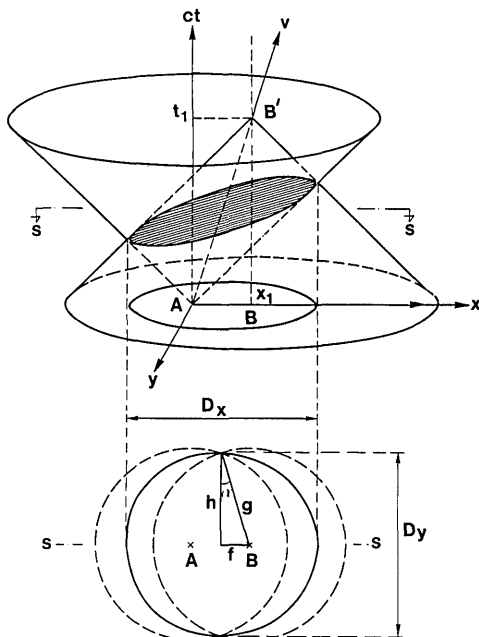
Fig. 3. Illumination and observation cones are separated both in time and space. One picosecond pulse is emitted at (O,O,O), and one picosecond observation is made at (x_1,O,t_1). At the intersection ellipse light is scattered by objects into the observation cone. When projected to the x-y plane, this ellipse produces one of the ellipses of the ordinary static holodiagram. If, however, the separation of emittance and observation is not static (x_1) but dynamic (vt_1), caused by a traveling observer, the projected intersection ellipse represents a relativistic effect. The desensitizing factor, halfway between A and B, is the same in the two cases and produces identical results, but in holography it is referred to as a trigonometric factor, while in relativity it is referred to as a transverse Doppler shift.

III. Cones Separated in Time and Space

A. Out of Contact

1. Static

If A and B are separated too far in space or too close in time $(x_1 > ct_1)$, the light cone and the observation cone will not meet at all (Fig. 1). In our 3-D world this situation corresponds to that observation made before the light pulse has reached the observer, which therfore sees no light at all.

2. Dynamic

The static separation in space of A and B is zero, but a dynamic separation is caused by a constant high velocity (v) in relation to a fixed space of the person who emits the light pulse and makes the observation. Thus, if we go back to Fig. 1, both the source of the short light pulse (point of illumination (A) and the point of observation (B) are at zero distance when the pulse is emitted at the coordinates (O,O,O). However, the observer travels with velocity v along the x axis, which corresponds to the observer moving along a straight line from A to B in Fig. 1. When observation takes place the coordinates of B' are (vt_1,O,t_1). Referring to Einstein's special theory of relativity, the speed

of light in vacuum always appears to have the constant value of c, therefore the light cone and the observation cone are (when studied from our stationary world) in no way influenced by the velocity of A and B. Thus the evaluation based on the two cones is, in the case of a dynamic separation, identical to that already described for static separation.

Let us point by point compare this situation to the static one described in Sec. III. A.1, where the two cones do not meet at all. In our 3-D world that situation corresponds to the velocity of the observer being faster than the speed of light, so that the observation can be made before the light arrives. Referring to the basis of Einstein's special theory of relativity, such a velocity does not exist. For the studied dynamic separation, the situation of Fig. 1 is therefore impossible, the angle separating the line A–B' from the ct axis must always be smaller than 45°.

B. Tangential line

Let us now keep the time separation of A and B' constant, but step by step move B toward A and study what will happen. As the two cones touch each other, B' will see a flash of light in the direction of A.

1. Static

In our ordinary 3-D world this means that the observer makes his observation just as the spherical wavefront of the pulse from A passes B'.

2. Dynamic

In our dynamic case this situation indicates that B' travels with the same speed as the pulse $(v = c)$.

C. Intersecting Cones

If we move B still closer toward A, again no light is observed, this time because B makes the observation too late; the spherical light pulse from A has already passed. However, as the apex of the light cone now is inside the observation cone and vice versa, the two cones intersect because $x < ct$ (Fig. 3). If there are scattering particles everywhere in space, or even some larger surfaces, light might be scattered from the light cone into the observation cone. As this can happen only on the surfaces of the cones, only those particles and those objects situated where the two cones intersect can be seen from B. The line of intersection forms an ellipse on a plane, the inclination of which decreases from 45° to 0° as the distance A–B decreases toward zero. At the same time the eccentricity of the ellipse decreases too, until the situation is identical to that in Fig. 2. The intersection ellipse is tilted because the observer sees different objects at different points of time. It is interesting to note that this inclined ellipse is flat, which proves that there is a linear relationship between x and t along the intersection line.

The projection of the inclined intersection ellipse of Fig. 3 down to the x-y plane produces another ellipse, its focal points being A and B, respectively. This ellipse is one of the ellipses of the holodiagram.
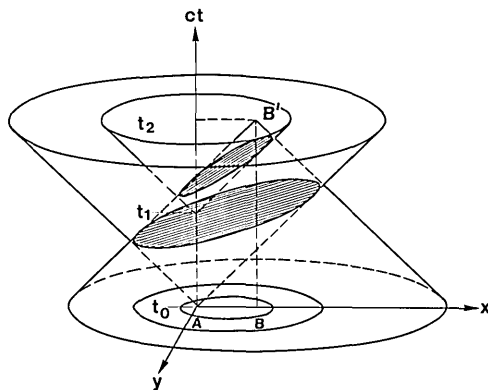
Fig. 4. Differences between the static and the dynamic holodiagram are revealed when more than one picosecond pulse is studied. In this figure the separation of A and B is static and therefore the intersection ellipses, when projected down to the x-y plane, represent the total ordinary static holodiagram. They all have the two common focal points A (illumination) and B (observation). The smallest ellipses have the largest eccentricity and their corresponding intersection ellipses have the largest tilt.

1. Static (holography)

Let us now study the situation when A emits first one pulse at (O,O,O), then with a separation of dt, a second pulse is emitted at (O,O,t_1), and finally the observation is made after another delay of dt at B (O,O,t_2), as seen in Fig. 4. Two intersecting ellipses are formed, the one closest to B is smallest but has the largest eccentricity and the largest tilt.

If A finally, produces not only two pulses but a train of pulses at the constant intervals dt, a set of concentric intersection ellipses will be produced where those that are innermost have the largest eccentricity and also the largest inclination in relation to the x-y plane. When projected down to the x-y plane, they will all have their focal points at A and B. The separation of the ellipses in the x-y plane will (along the x axis and outside A–B) be constant and have the value $0.5c\ dt$. At all other points in the x-y plane this separation will be larger, and we will designate it $k = 0.5c\ dt$, where k is the k value of the holodiagram (Fig. 5).

In our 3-D world these ellipses represent the cross section through the axis of rotation A–B of a set of rotational symmetric ellipsoids that represent constant path lengths for light that is transmitted from A to B via points on the ellipsoidal surfaces. To simplify the situation let us go to the 2-D ellipses of the holodiagram (Fig. 5) and, to visualize the function of these ellipses, let us paint black every second area between adjacent ellipses (Fig. 6).

2. Dynamic (Relativity)

If we start with Fig. 1 and then move B closer to A, by decreasing the velocity, the situation will be identical to that of Fig. 3, as already described for the static case (Sec. III. C.1). The line of intersection forms an ellipse on a plane the inclination of which decreases from 45° to 0° as the distance A–B decreased toward zero (the velocity of the observer B' decreases to zero). At the
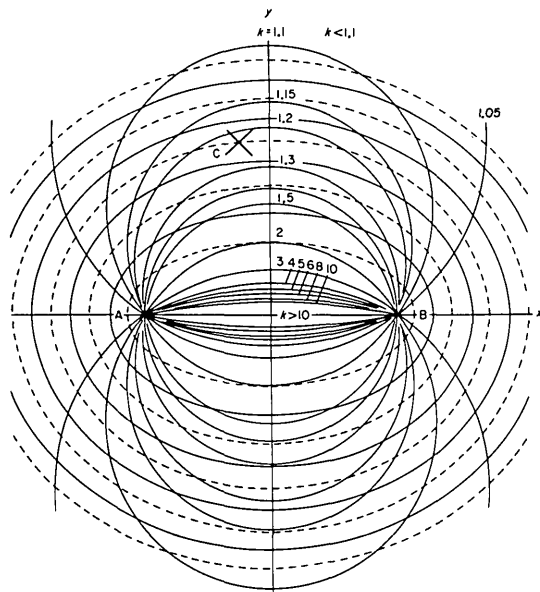

Fig. 5. Static holodiagram as derived from Fig. 4. When used in holographic interferometry, A is the point from which the divergent laser beam originates, while B is the point of observation behind the hologram plate. Light from A scattered to B by the object at C will not change its path length if C is displaced along an ellipse, while the difference in path lengths to adjacent ellipses is a constant number of wavelengths. The displacement perpendicular to the ellipses needed to cause one fringe is $k\ 0.5\lambda$, where k is constant along arcs of circles, each representing a different spacing of the ellipses.
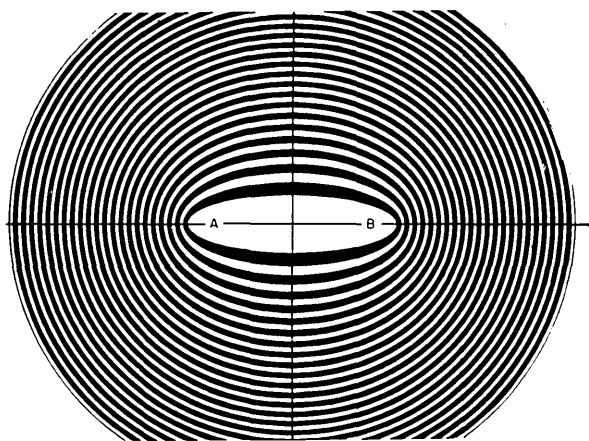

Fig. 6. To visualize the ellipses of the static holodiagram we have drawn a number of closely spaced ellipses with the common focal points A and B. Every second elliptic area between adjacent ellipses was painted black, so that the thickness of black-and-white areas represents the k value and thus the interferometric sensitivity to displacement. If two transparencies are made of this figure and one is displaced in relation to the other, moire fringes are formed that correspond to the interference fringes caused by that displacement.

same time the eccentricity of the ellipse decreases too, until the situation is identical to that in Fig. 2.

The projection of the inclined intersection ellipse down to the x-y plane produces another ellipse, its focal points being A and B, respectively. This ellipse is identical to one of the ellipses of the holodiagram.
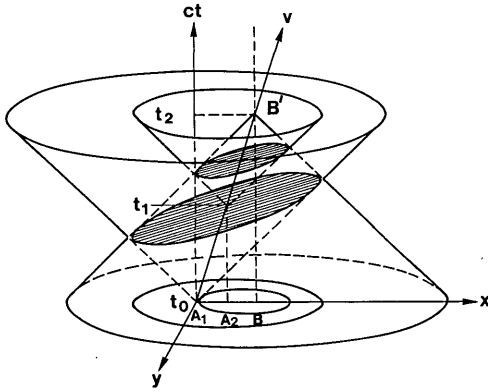
Fig. 7. Dynamic holodiagram. In contrast to that of Fig. 5 the distances along the x axis are solely caused by a constant velocity in the x direction by the person who makes the observation. He emits the first picosecond pulse at (O,O,O), the second at (vt_1,O,t_1) and finally he makes the single picosecond observation at (vt_2,O,t_2). When the intersection ellipses are projected down to the x-y plane, it is found that they all have one common focal point at B, but the other focal points $(A_1, A_2,$ etc.) are different for each ellipse. In contrast to the static holodiagram of Figs. 5–7 it is also found that all the ellipses have the same eccentricity and that all the intersection ellipses have the same inclination. The k lines of the static holodiagram are in this dynamic holodiagram substituted by q lines that are constant, no along circles through B, but along straight lines through B.

Fig. 8. Traveling observer moves at constant speed $(0.6c)$ to the right and emits picosecond pulses at A_1, A_2, etc. separated by vdt. His lines of sight are aberrated from angle γ to the angles drawn in this dynamic holodiagram (the q lines). Along each q line the separation of the intersections by the ellipsoids of observation have a constant value, the q value. Doppler shift, apparent speed of time, and apparent longitudinal magnification are all functions of q, while transversal Doppler shift, time dilation, and Lorentz contraction depend only on the q line representing $\gamma = 90°$.

Thus the moving observer's spheres of observation, because of his velocity, are transformed into these ellipsoids of observation in the stationary frame of reference (the x-y plane). The eccentricity (e), which is identical to the relationship between the major axis of the ellipsoid and the radius of the sphere, results in the distances along the x axis of the stationary world to the traveler appearing foreshortened. Thus the well-known Lorentz contraction is equal to the inverted value of the eccentricity.

Referring to Fig. 3 we show how this eccentricity is calculated and how the static (k) and the dynamic (q) desensitizing factors are derived:

static:

$$k = \frac{1}{\cos\alpha} = \frac{g}{h} = \frac{0.5D_x}{0.5D_y} = e. \tag{1}$$

dynamic:

$$q = \frac{1}{\cos\alpha} = \frac{g}{h} = \frac{0.5D_x}{0.5D_y} = e = \frac{g}{\sqrt{g^2-f^2}} = \frac{1}{\sqrt{1-\left(\frac{v}{c}\right)^2}}. \tag{2}$$

3. Static and Dynamic Holodiagram

Until now the static and dynamic situations produced identical results concerning the ellipses of intersection and the corresponding ellipsoids of our 3-D world, as seen in Fig. 3. In the following we show the characteristics of each.

If A emits not only one single pulse but a train of pulses at constant time intervals dt (which because of the constant velocity correspond to constant space intervals dx), a set of concentric intersection ellipses is
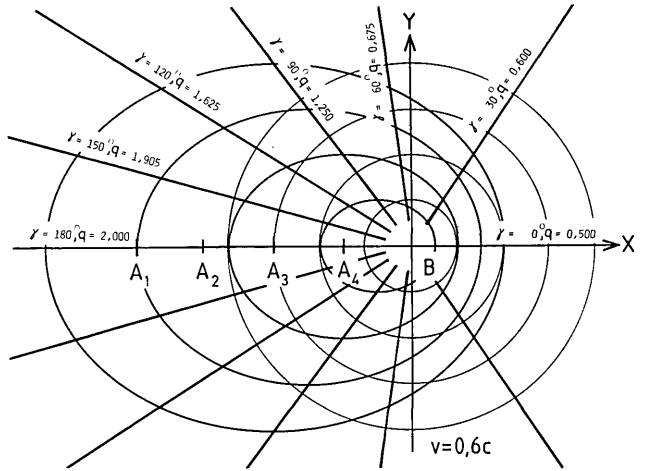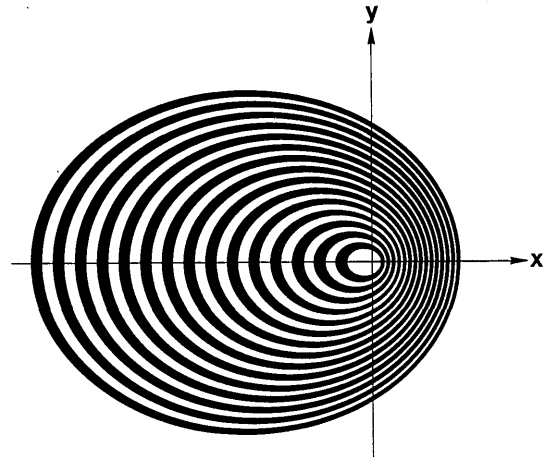

Fig. 9. To visualize the ellipses of the dynamic holodiagram we have drawn a number of closely spaced ellipses all derived from the projected intersection ellipses as described in Fig. 7. Just as in the static diagram of Fig. 6 every second elliptic area between adjacent ellipses was painted black. The separation of these ellipsoids of observation divided by the separation of the ordinary spheres of observation corresponding to zero velocity represents the q value.

produced. However, in contrast to those of the conventional static holodiagram the whole set of ellipses of this new dynamic holodiagram has the same eccentricity and also the same inclination in relation to the x-y plane (Fig. 7). When projected down to the x-y plane, they all have one common focal point at B, while their respective focal points A are separated by the distance $dx = v \, dt$ (Figs. 8 and 9). The separation of the ellipses (s) in the x-y plane along the x-axis to the right of B (in

front of the observer) is smaller than the separation corresponding to zero velocity (s), while it is larger than s behind the observer. At all other points in the x-y plane the separation varies between these two values, and we designate it qs.

Thus we could say that the k value of the static holodiagram (Fig. 5) represents the relation between the separation of the ellipses of Fig. 6 compared with the separation of the spheres corresponding to zero distance between A and B. In a similar way we could say that the q value of the dynamic holodiagram (Fig. 8) represents the relation between the separation of the ellipses of Fig. 9 compared with the separation of the spheres corresponding to zero velocity. However, in the dynamic holodiagram the separation of the ellipses should be measured along the (aberrated) lines of sight from the observer at B.

In the static holodiagram (Fig. 5) the innermost ellipses have infinite eccentricity (infinite k value), while the outermost ellipses asymptotically become spheres (k value equal to one). The k value is constant along arcs of circles through A and B (Fig. 5). Its value at C is

$$k = \frac{1}{\cos\alpha}, \tag{3}$$

where α = half of the angle ACB. In the dynamic holodiagram (Fig. 8), on the other hand, for a certain velocity the eccentricity is constant for all ellipses, thus they are all identical and vary only in size. Therefore the q value is constant along straight lines that radiate from the common focal point B. The q value at a certain angle is referred to in Fig. 10:

q = the distance BG divided by the distance BK,

or

$$q = \frac{1 - \frac{v}{c}\cos\gamma}{\sqrt{1 - (\frac{v}{c})^2}}. \tag{4}$$

IV. Uses of the Static Holodiagram

A. Optimization

The static holodiagram can be used to optimize the utilization of a limited coherence length and to evaluate the sensitivity of conventional and holographic interferometry.[1]

B. Measuring Pulse Length Using Light-in-Flight Recording by Holography

Let the difference in path length corresponding to two adjacent ellipses represent the pulse length (ct) of a laser (A) used for making a holographic recording at B. Then, the bright fringe seen in the reconstructed holographic image of an object (C) represents its intersection by the area between those two adjacent ellipses, the separation (s) of which is

$$s = k\,0.5ct. \tag{5}$$

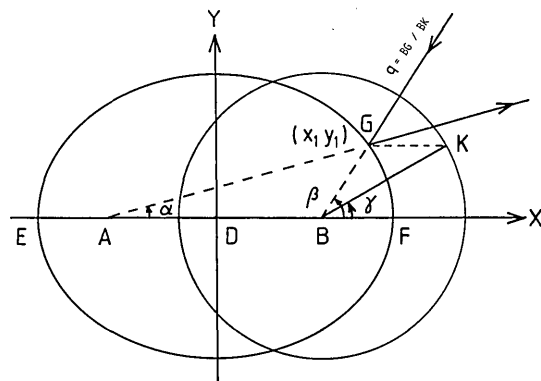Now let us measure the pulse length by introducing a

Fig. 10. To the traveling observer an arbitrary point G of the stationary world appears to exist at K which is found by drawing a line of constant Y value from G to the sphere. Light rays emitted by the traveler at angle γ are aberrated by his velocity to angle α, while his lines of sight are aberrated from angle γ to angle β. This is the method used to produce both Figs. 8 and 11.

ruler, with, e.g., one division per millimeter, into the scene that is recorded by the hologram. This ruler will then, in the reconstructed holographic image, be seen illuminated by one bright fringe representing its intersection by the separation of two ellipsoids. To get the true pulse length we tilt the ruler until we get the shortest possible reading of the illuminated part. In this way we make sure that we measure in a direction that is perpendicular to the apparent pulse front and that we therefore measure the correct value of the apparent pulse length. Thus the apparent pulse length (L_{app}), as represented by the bright fringe, seems to be half of its true value (L_{true}) at the x axis to the right of B and to the left of A. Everywhere else it appears to be longer. At the x axis in between A and B it appears to be infinitely long. The true temporal pulse length (t_{true}) will be

$$t_{true} = L_{app}/k\,0.5c. \tag{6}$$

C. Measuring Pulse Velocity

The pulse velocity appears to be half of that of light at the x axis to the right of B and the left of A. Everywhere else it appears to be faster. At the x axis in between A and B the apparent pulse velocity (v_{app}) is infinitely higher than the speed of light:

$$v_{app} = k\,0.5c. \tag{7}$$

The pulse shape appears distorted. The originally spherical pulse front around A appears transformed into one of the ellipsoids of the holodiagram. A flat wavefront appears transformed into another 3-D equivalence to a conical section, a paraboloid.

D. Measuring the 3-D Shape of Objects Using Light-in-Flight Recording by Holography

The setup is identical to that of the last example. However, instead of measuring the pulse itself we use the pulse as a ruler to measure 3-D objects. Because of the already discussed apparent distortions of the pulse, we get the following results:
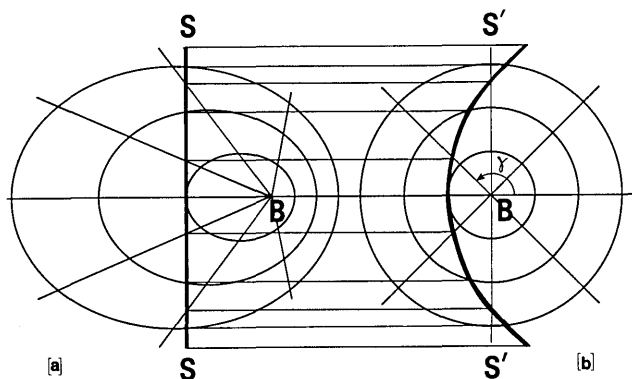
Fig. 11. Flat surface (s–s) perpendicular to the direction of travel appears distorted to the traveling observer (B) into the curved surface s'–s', which is constructed in the following way: Draw lines parallel to the x axis from the points where s–s intersects the ellipsoids of observation until they reach corresponding points on the spheres of observation. The same can be done going from the intersections with the aberrated lines of sight (q lines) to the original lines of sight (at angle γ). Connecting these points results in the traveler's impression s'–s' of the stationary surface s–s. (a) Ellipsoids of observation and aberrated lines of sight; (b) spheres of observation and original lines of sight.

$$L_{true} = L_{app}\,0.5k. \qquad (8)$$

Because of the different apparent velocity of light at different locations in the diagram, the definition of simultaneity is changed and, as the spherical wavefronts appear elliptical, the measured apparent shape of objects will change.

V. Uses of the Dynamic Holodiagram

A. Transformations from Spheres to Ellipsoids

Using simple trigonometry and the transformations of Figs. 8–10 produces the following results:

(1) The apparent length (L_{app}) compared with the true length (L_{true}) of object dimensions measured parallel to the line of travel is

$$L_{app} = \frac{1}{q}\,L_{true}. \qquad (9)$$

Thus objects coming toward the observer appear longer, while those moving away appear shorter. Only as they are just passing by (with an observation angle of 90°) do they appear Lorentz contracted.

(2) The wavelength of light (λ_{true}) from moving objects appears Doppler shifted into xx. Thus,

$$\lambda_{app} = q\lambda_{true}. \qquad (10)$$

Therefore, when interferometry is used,

$$L_{app} = \frac{1}{q}\,L_{true}. \qquad (11)$$

B. Distortions of an Orthogonal Coordinate System

Finally we use the graphic method of Fig. 11 to study the transformation of an orthogonal coordinate system (Fig. 12). The traveling observer (B) passes as before from left to right with the speed of $0.6c$ through the stationary world. Figure 11(b) shows the travelers spheres of observation and his lines of sight. In Fig. 11(a) we see how, in relation to the stationary world, his lines of sight are aberrated and his spheres are transformed into ellipsoids. Let us study one stationary straight line that is perpendicular to the direction of travel and see how it appears distorted to the traveling observer.

From every point at which the studied stationary line of Fig. 11(a) is intersected by an ellipsoid or by an aberrated line of sight, a horizontal line is drawn to Fig. 11(b), until it intersects the corresponding sphere or the corresponding (unaberrated) line of sight. The curve connecting these intersections in Fig. 11(b) then represents the straight line of Fig. 11(a) as it appears distorted to the traveling observer.

In Fig. 12(a) a total stationary orthogonal coordinate system is shown and in Fig. 12(b) we see the corresponding distorted image as observed by the traveler, represented by the small circle ($i,O,$) passing from left to right. The identical transformation would occur if the observer at B were stationary and instead the orthogonal coordinate system were passing him with the constant speed of $0.6c$ from right to left.

All apparent displacements are caused by the fact that different points on the object are studied at different points in time. During this time difference the object has moved in relation to the observer, but only along its line of motion. Thus, flat surfaces perpendicular to the direction of the velocity are distorted into
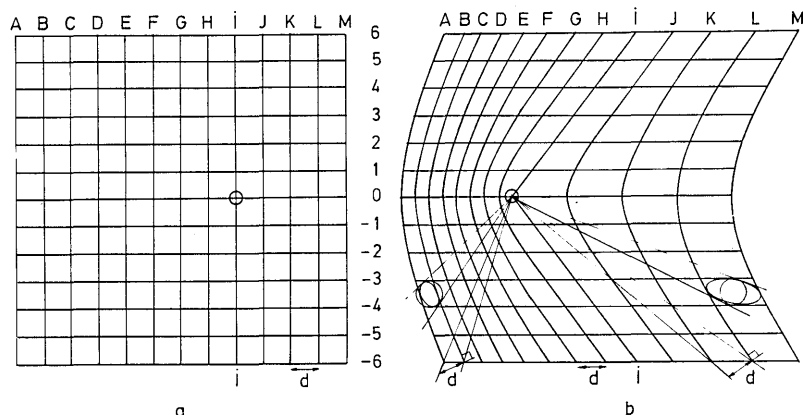

Fig. 12. Orthogonal coordinate system of the stationary world (a) appears to the traveling observer transformed into that of (b). The traveler exists at the small circle (i,O) and is moving to the right at a speed of $0.6c$. This situation is identical to that when the observer is stationary while the coordinate system is moving to the left. From the diagram we find that flat surfaces are transformed into hyperboloids. The plane (i–i) through the observer is transformed into a cone. The back side can be seen on all objects that have passed this cone. The separation of advancing hyperboloids is increased, while that of those moving away is decreased.

hyperboloids, while those that are parallel to the motion are not changed with respect to flatness, angle, or separation. This fact can also be understood from Fig. 3 where all the distortions result from the tilt of the intersection planes of the two cones. This tilt is caused by the separation of B from A which in turn is caused by the velocity of B along the x axis. Because of symmetry the tilt axis is parallel to the y axis, along which it consequently produces no distortion.

VI. Conclusion

By studying the intersection of light cones we have derived in a new way the ordinary static holodiagram that can be used for conventional or holographic interferometry. We have also shown how it can be used to explain the apparent distortions of time and space when wavefronts are studied, e.g., using light-in-flight recordings by holography. Thus it is our belief that the Minkowski diagram will also become an important tool in ordinary interferometry and especially in holography with picosecond pulses. To be able to evaluate such ultrahigh-speed movies it is necessary to compensate for the distortions caused by the limited speed of light.

Just as the Minkowski diagram, intoduced to explain relativistic effects, can assist in the understanding of holographic phenomena, the holodiagram, introduced to explain holographic effects, can assist in the understanding of relativistic phenomena. Therefore we have introduced the modified dynamic holodiagram and demonstrated how it can be used to visualize in a graphic way relativistic apparent distortions. Good agreement was found when we compared these results with our earlier work[2,3] and with those published by a number of physicists working in the field.[7-10] However, in this paper we do not pretend to distinguish between apparent and true distortions. We hope that our work has built a bridge between the conventional static optics and the optics of ultrafast exposures and of ultrahigh velocities which will become more and more important as picosecond and femtosecond pulses find more general use as measuring tools.

References

1. N. Abramson, *The Making and Evaluation of Holograms* (Academic, London, 1981), pp. 28, 110, 144, and 197.
2. N. Abramson, "Light-in-Flight Recording. 3: Compensation for Optical Relativistic Effects," Appl Opt. 23, 4007 (1984).
3. N. Abramson, "Light-in-Flight Recording. 4: Visualizing Optical Relativistic Phenomena," Appl. Opt. 24, 3323 (1985).
4. A. Einstein, *The Meaning of Relativity* (Methuer & Co LTD, 1950), p. 36.
5. A. Einstein *et al.*, *The Principle of Relativity* (Dover, New York, 1952), p. 73.
6. N. Abramson, "Light-in-Flight Recording: High-Speed Holographic Motion Picture of Ultrafast Phenomena," Appl. Opt. 22, 215 (1983).
7. R. Bhandari, "Visual Appearance of a Moving Vertical Line," Am. J. Phys. 38, 1200 (1970).
8. J. Terell, "Invisibility of the Lorentz Contraction," Phys. Rev. 116, 1041 (1959).
9. P. M. Mathews and M. Lakshmanan, "On the Apparent Visual Forms of Relativistically Moving Objects," Il Nuovo Cimento 12, 168 (1972).
10. G. D. Scott and H. J. van Driel, "Geometrical Appearances at Relativistic Speeds," Am. J. Phys. 38, 971 (1970).

Preach, my dear Sir, a crusade against ignorance; establish

and improve the law for educating the common people. Let

our countrymen know that the people alone can protect us

against these evils, and that the tax which will be paid

for this purpose is not more than a thousandth part of what

will be paid to kings, priests, and nobles who will rise up

among us if we have the people in ignorance.

T. Jefferson, 1786